Available online at www.sciencedirect.com
SCIENCE DIRECT
Polymer 46 (2005) 12539–12545
polymer
www.elsevier.com/locate/polymer

Creep and physical aging behaviour of PA6 nanocomposites

D.P.N. Vlasveld [a,b], H.E.N. Bersee [c], S.J. Picken [a,b,*]

[a] Polymer Materials and Engineering, Faculty of Applied Sciences, Delft University of Technology, Julianalaan 136, 2628 BL Delft, The Netherlands
[b] Dutch Polymer Institute, John F. Kennedylaan 2, P.O. Box 902, 5600 AX Eindhoven, The Netherlands
[c] Design and Production of Composite Structures, Faculty of Aerospace Engineering, Delft University of Technology, Kluyverweg 3, P.O. Box 5058, 2600 GB Delft, The Netherlands

Received 23 June 2005; accepted 25 October 2005
Available online 14 November 2005

Abstract

The creep and physical aging behavior of various types of PA6 nanocomposites and unfilled PA6 are described. After annealing far above T_g the samples were quenched to room temperature and tested after various ageing times. The creep compliance shows a significant reduction with the addition of exfoliated layered silicate to the matrix polymer. The shape of the creep curves of the nanocomposites is similar to unfilled PA6 and time—ageing time superposition is possible with all materials. The shift rate for superposition is in the same range, but slightly higher in nanocomposites. The creep behavior of nanocomposites conditioned with an equilibrium amount of moisture and dry samples at elevated temperatures shows that the effect of nanofillers is much stronger under these conditions.

Keywords: Nanocomposite; Creep; Physical aging

1. Introduction

Creep is the time dependent deformation of materials subjected to a continuous stress. This deformation can be both elastic and plastic, and therefore, it can be non-recoverable when the load is removed. Creep can lead to unacceptable deformation and eventually even to structural failure and is, therefore, a very important property for engineering plastics and composites. The creep response is quantified by the creep compliance, which is the strain divided by the applied stress.

In polymers, the deformation process under load is strongly dependent on the mobility of the chains. The chain mobility is not only temperature dependent, but also time dependent. The time dependent change of the properties in amorphous polymers below T_g is known as physical aging [1]. The physical aging process is driven by the difference between the actual volume and the thermodynamic equilibrium volume of an amorphous polymer when it is quenched from a temperature above T_g to below T_g. Upon fast cooling below T_g the polymer cannot shrink fast enough to keep the equilibrium volume due to the low chain mobility. Therefore, during extended aging periods the polymer slowly evolves towards this equilibrium situation. The physical aging process results in property changes such as an increase in density, modulus and yield stress, and a reduction in ductility, ultimate elongation and creep rate.

In semi-crystalline polymers the physical aging behavior of the amorphous phase is more complex. It has been shown that physical ageing also occurs well above T_g of the amorphous phase in semi-crystalline polymers [1–9]. An explanation for this extended temperature range at which ageing occurs was proposed by Struik [1,4–6], and involves a range of different amorphous phases. In general, the model assumes that amorphous polymer close to a crystalline region or filler particle has a reduced mobility and therefore a higher T_g. Further from the rigid phase, the T_g decreases towards the bulk T_g. This results in the broadening of the loss modulus peak compared to purely amorphous polymers as is seen in dynamic mechanical measurements. In the simplified Struik-model two different T_g's are assumed instead of a continuous range: one for the bulk amorphous material and one for the material with a reduced mobility. The aging behavior below the lowest (bulk) T_g (region 1) is similar to the behavior in amorphous polymers. Struik [1] has shown that at low deformations

* Corresponding author. Address: Polymer Materials and Engineering, Faculty of Applied Sciences, Delft University of Technology, Julianalaan 136, 2628 BL Delft, The Netherlands. Tel.: +31 15 278 6946; fax: +31 15 278 7415.
E-mail address: s.j.picken@tnw.tudelft.nl (S.J. Picken).

0032-3861/$ - see front matter © 2005 Elsevier Ltd. All rights reserved.
doi:10.1016/j.polymer.2005.10.120

(in the linear visco-elastic regime) and below T_g the creep curves for different ageing times can be superimposed on one reference ageing time by shifts along the time axis. A commonly used method to describe the aging behavior is to plot the shift factor a_{t_e} versus the aging time t_e on a double logarithmic plot and determine the slope. The slope μ (Eq. (1)) in the plot of $\log(a_{t_e})$ versus $\log(t_e)$ is known as the shift rate [1].

$$\mu = \frac{d\log(a_{t_e})}{d\log(t_e)} \tag{1}$$

Measurement of the creep rate at different ageing times can be performed on the same sample if the stress is small enough to prevent permanent deformation. The testing time should be less than 10% of the ageing time to minimise the effect of ageing during the measurement.

Polyamide 6 (PA6) nanocomposites containing exfoliated layered silicate particles have been developed to improve the mechanical properties, and to reduce the flammability and moisture permeability. Due to the large aspect ratio and the high stiffness of the particles, the optimal properties are reached at lower filler content than with the use of traditional mineral or fiber fillers. Because of the increased modulus of nanocomposites, it can be expected that the creep is also reduced. However, to the best of our knowledge hardly any data has been published so far for nanocomposites on this important subject. The physical aging behavior also remains to be investigated for nanocomposites. It is interesting to see if the reduced ductility and elongation at break of nanocomposites could have a connection with a modified physical aging. Extensive research has been done previously on the physical ageing of unfilled polyamides, for example, on PA6 [1] and PA66 [3]. The results revealed a complex behavior dependent on ageing temperature and applied stress. Annealing temperatures of 150–160 °C were used for the thermal rejuvenation of the PA6 and PA66 samples before quenching to the ageing temperature, and for the applied stress usually less than 25% of the yield stress was used. For (dry) PA6 the double logarithmic shift rate μ at room temperature was found to be around 0.75 [1].

Measurement of the creep is a very practical method to study the physical aging phenomenon, and in creep studies the influence of physical aging needs to be considered for a correct interpretation of the data. Therefore, the phenomena of creep and physical aging in PA6 nanocomposites are investigated together in this paper. PA6 reference materials (low and high molecular weight) are compared with melt-exfoliated nanocomposites with a range of silicate concentrations. In addition, a commercially available in situ polymerized nanocomposite and a nanocomposite containing unmodified (water-swellable) silicate have been investigated. Samples annealed far above T_g (160 °C) were quenched to room temperature and tested after various ageing times. Some tests were done at 80 °C and on moisture conditioned samples to investigate the influence of increased polymer mobility on the creep behavior.

2. Experimental

2.1. Materials

2.1.1. Polyamide 6, low molecular weight (LMW PA6)

Akulon® K222D, injection-moulding grade PA6 from DSM, the Netherlands.

$M_n \approx 16{,}000$, $M_w \approx 32{,}000$ g/mol, $T_m \approx 220$ °C.

2.1.2. Polyamide 6, high molecular weight (HMW PA6)

Akulon® K136, film/extrusion grade PA6 from DSM, the Netherlands.

$M_n \approx 35{,}600$, $M_w \approx 71{,}000$ g/mol, $T_m \approx 220$ °C.

2.1.3. Commercially available PA6 nanocomposite

Unitika M1030D, from Unitika, Japan. This nanocomposite with 4.6 wt% silicate is produced by in situ hydrolytic polymerisation of ε-caprolactam in the presence of swollen organically modified silicates. The organic surfactant is the initiator for polymerisation, so the polymer chains are bound to the surfactant via covalent bonds. The surfactants have an ionic bond with the silicate layers and this way the polymer is ionically bound to the silicate layers, unlike melt-processed nanocomposites, which rely on H-bonding and dipolar interactions.

2.1.4. Organically modified layered silicate

Somasif® MEE (Synthetic Mica®) from Co-op Chemicals, Japan.

This is synthetic fluorine mica, covered with a methyl bis-2-hydroxyethyl coco quaternary ammonium surfactant (28.5 wt%, determined with a Perkin–Elmer TGA-7 Thermal Gravimetric Analyzer at 800 °C for 1 h in air).

2.1.5. Unmodified layered silicate

Somasif® ME-100 (Synthetic Mica®) from Co-op Chemicals, Japan.

This is water-swellable synthetic fluorine mica, which does not contain any organic surfactant; it is the inorganic basis of Somasif® MEE.

2.2. Sample preparation

2.2.1. Extrusion

The nanocomposites with Somasif® MEE were prepared by mixing the layered silicate with PA6 (K222D) in a Werner and Pfleiderer ZDS-K28 co-rotating twin-screw extruder. The extruder was operated at a screw speed of 200 rpm and a feeding rate of approximately 3 kg/h. The temperature in the feeding zone was 150 °C, all the other zones where heated to 230 °C. Cooling was applied to keep the temperature constant since the high shear forces in the melt can produce too much heat. First a master batch with 11 wt% (based on the inorganic content of the filler) was made and the lower concentrations were made by diluting the master batch with PA6 in a second extrusion step.

The nanocomposites with Somasif® ME-100 were made by feeding a mixture of cryogenically milled PA6 (K222D) and ME-100 powder in a Werner and Pfleiderer ZSK 30/44 D co-rotating twin-screw extruder. To enhance the exfoliation of the water-swellable ME-100 silicate, water was injected into the extruder at a rate of 25 ml/min, and removed by venting at the end of the extruder. The extruder was operated at a temperature of 240 °C at a rotation speed of 200 rpm and a feeding rate of approximately 10 kg/h.

2.2.2. Injection moulding

Dumbbell shaped samples according to the ISO 527 standard were injection moulded on an Arburg Allrounder 221-55–250 injection-moulding machine. The feeding zone was heated to 150 °C, the melting and mixing zones heated to 240 °C and the nozzle was kept at 260 °C.

2.2.3. Annealing

Dry as moulded samples were annealed in a vacuum oven at 160 °C for 15 h before quenching to the aging temperature. Subsequently the samples were taken from the vacuum oven and immediately stored in a desiccator containing a $CaCl_2$ drying agent, in an air-conditioned room at 23 °C.

2.3. Testing

2.3.1. Silicate content

Thermogravimetric analysis (TGA) measurements were done to determine the exact silicate content in the tested samples after processing. A Perkin–Elmer TGA-7 thermal gravimetric analyzer was used to determine the weight fraction of silicate by heating a sample in air at 800 °C for 1 h.

2.3.2. Creep

The samples were tested on a Zwick 1445 tensile tester with a 10 kN force cell. The test machine was equipped with a force feedback loop to be able to test at a constant stress. A constant stress of 16 MPa was used in all ageing experiments, which is approximately 1/5 of the yield stress. This stress was reached and stabilized within 20 s after the start of the loading. The loading period was never longer than 10% of the previous ageing time, to reduce the influence of ageing during the test. The temperature of the test equipment and the samples during the ageing and creep tests was maintained at 23 ± 0.5 °C by air-conditioning of the room containing the samples and test equipment. The samples were tested inside a climate chamber on the tensile tester, which was flushed with dried air to prevent moisture uptake during the creep tests. After each creep test the samples were stored again in the desiccator to prevent moisture absorption during ageing.

3. Results and discussion

In Figs. 1–7 the results are displayed for all the creep tests on the various materials at different ageing times. The creep compliance (strain/stress) in GPa^{-1} is shown on the vertical axis on a linear scale and the time is shown on a logarithmic scale. For clarity, the curves that are shown are obtained from a polynomial fit through the original data, which removes fluctuations due to small inaccuracies in the measurement. The Kohlrausch–Williams–Watts equation that can describe the ageing behavior of amorphous polymers [1,3] could not describe every creep curve in our materials accurately enough and, therefore, a polynomial fit of the form $y = a + b \ln t + c \ln^2 t + d \ln^3 t + e \ln^4 t$ (y = compliance, t = time) was used instead. Although the constants in this equation have no physical meaning, the equations can describe all creep curves very accurately and it can be used to determine the slope of the curves. All measurements are performed at 23 °C in a dry environment, well below T_g of PA6.

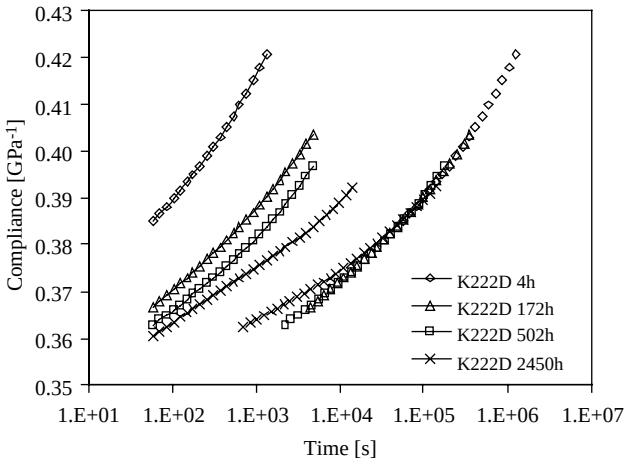

Fig. 1. Creep compliance for low MW PA6 (K222D) as a function of ageing time. The overlapped curves on the right are the curves shifted over the time axis onto one master curve.

In each of the Figs. 1–7 the creep curves for different ageing times can be superimposed on one reference ageing time by shifts along the time axis. The master curve is shifted by one decade from the longest ageing time for clarity. In all figures it can be seen that at the highest ageing time (770 h or higher, or approximately one month) the curves have a slightly different shape and that the superposition cannot be done very

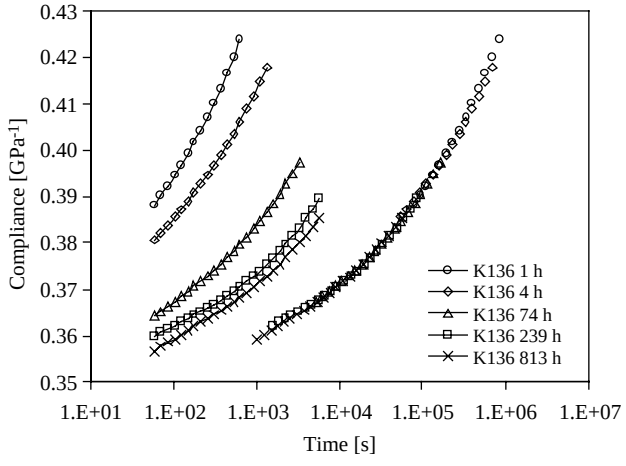

Fig. 2. Creep compliance for high MW PA6 (K136) as a function of ageing time. The overlapped curves on the right are the curves shifted over the time axis onto one master curve.

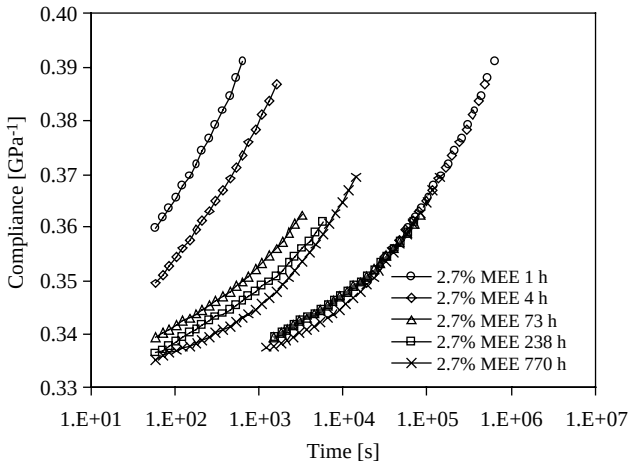

Fig. 3. Creep compliance for 2.7% MEE nanocomposite as a function of ageing time. The overlapped curves on the right are the curves shifted over the time axis onto one master curve.

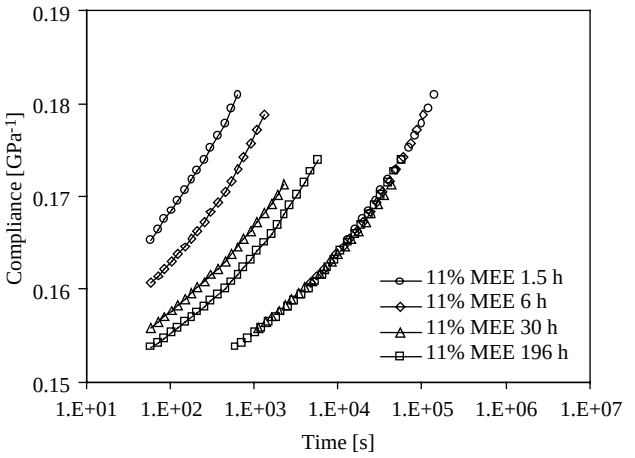

Fig. 5. Creep compliance for 11% MEE nanocomposite as a function of ageing time. The overlapped curves on the right are the curves shifted over the time axis onto one master curve.

accurately. In Figs. 1 and 2 the results for two types of unfilled PA6 can be seen. There is virtually no difference in the level of the creep compliance between the two different molecular weights. It shows that below T_g the molecular weight has little influence on the creep behavior, because only local motion of the chain segments is involved in the glassy state. Therefore, the creep results will not be influenced by possible differences in MW that might occur due to the processing of the nanocomposites. In Figs. 3–5 the creep results are shown for organically modified nanocomposites containing 2.7, 6 and 11 wt% silicate, respectively, Fig. 6 shows the results for a nanocomposite based on unmodified layered silicate and Fig. 7 for a commercial nanocomposite. The shape of the curves in the nanocomposite is very similar to those of the unfilled polymer, but the values of the creep compliance are much smaller.

In Fig. 8 the creep curves for the different materials after 4 h ageing time (6 h for 11% MEE) are collected, which clearly shows that nanocomposites containing more silicate have a lower creep compliance. A lower initial creep compliance can be expected, because the modulus increases with increasing silicate content (Fig. 9).

The modulus at the time that the stress of 16 MPa was first reached (20 s) shows an increase as a function of ageing time (Fig. 9). The increase is approximately linear when plotted versus the logarithm of time. To see if the creep rate is also reduced, besides the initial level of strain due to the higher modulus, the slope of the creep curves is calculated. To eliminate the effect of the differences in the initial compliance due to the differences in modulus, the compliance is normalized by dividing the compliance at time t by the initial compliance at time t_0 ($t=20$ s, when the maximum stress is first reached):

$$\frac{J_t}{J_0} = \text{normalized compliance} \tag{2}$$

The slope of the normalized compliance (SNC), shown in equation 3, is plotted in Fig. 10 for all materials after a 4 h ageing time (11% MEE after 6 h).

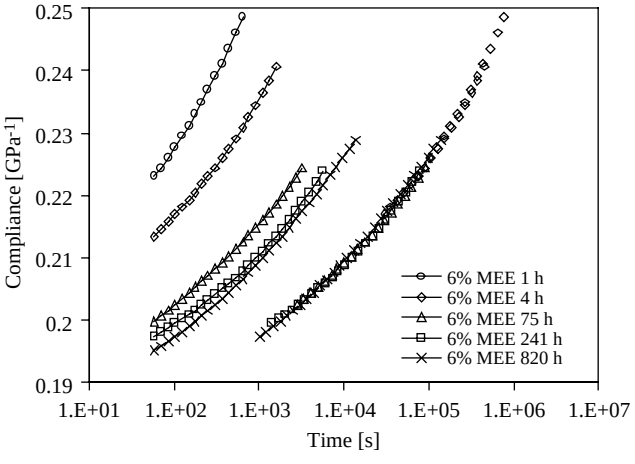

Fig. 4. Creep compliance for 6% MEE nanocomposite as a function of ageing time. The overlapped curves on the right are the curves shifted over the time axis onto one master curve.

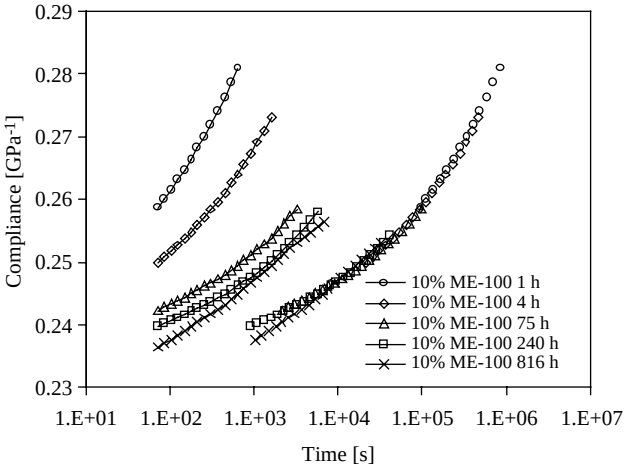

Fig. 6. Creep compliance for 10% ME-100 (unmodified silicate) nanocomposite as a function of ageing time. The overlapped curves on the right are the curves shifted over the time axis onto one master curve.

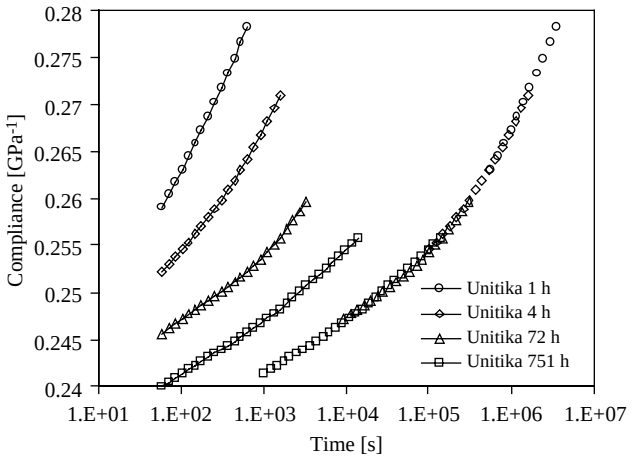

Fig. 7. Creep compliance for a commercial PA6 nanocomposite (Unitika M1030D) as a function of ageing time. The overlapped curves on the right are the curves shifted over the time axis onto one master curve.

$$\frac{d(J_t/J_0)}{dt} = \text{slope of the normalized compliance (SNC)} \quad (3)$$

The slopes of the normalized compliance (SNC) do not show a large difference between the nanocomposites and the unfilled PA6 (Fig. 10). The in situ polymerized nanocomposite (Unitika) seems to have a slightly lower SNC, which could indicate a faster ageing.

The logarithm of the shift factors a_{t_e} are plotted versus the logarithm of the aging time t_e on a double logarithmic plot in Fig. 11.

The slope of the curves in Fig. 11 determines the shift rate μ, as was shown in Eq. (1). The slopes are not changed much by the addition of layered silicate nanoparticles. The last points in the curves for the MEE nanocomposites, belonging to ageing times above 1 month, seem to deviate from the increase in a straight line. This could be a result of the equilibrium situation being approached, as was observed in glassy epoxy networks 5–10 °C below T_g [10]. However, because of the larger distance from T_g it is more likely that it is related to the change in curve shape observed at the longest ageing times, which makes time-ageing time superposition difficult (Figs. 1–7). When the last point clearly deviates, it is not used in the determination of

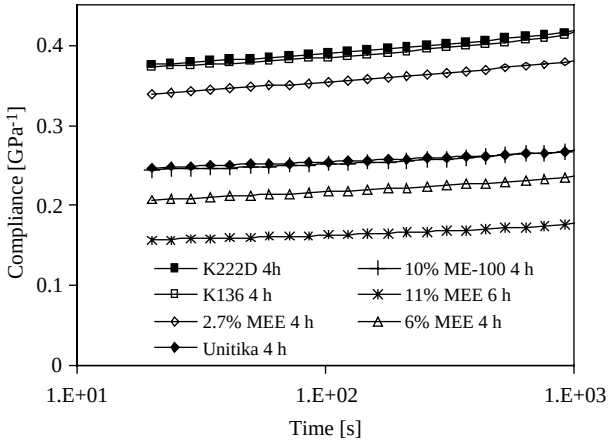

Fig. 8. Creep compliance after 4 h ageing for all materials.

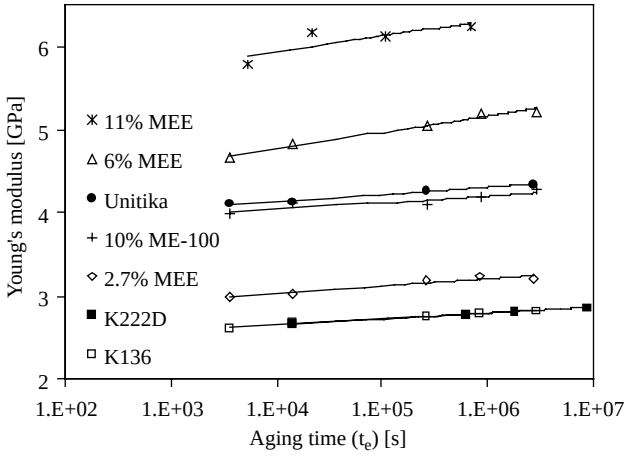

Fig. 9. Young's modulus as a function of various ageing time, calculated from the initial strain after 20 s, when the maximum stress of 16 MPa was just reached.

the shift rate. The shift rates (slopes) for all materials (Table 1) show a somewhat higher shift rate for the nanocomposites. The effect is not very large, and a difference between the two types of unfilled PA6 can be seen as well. The difference between the two unfilled PA6 samples is probably an indication of the margin of error, because both types of PA6 seem to show the same behavior in creep compliance (Fig. 1) and modulus (Fig. 9). The values between 0.70 and 0.76 for unfilled PA6 are in the same range that is measured by Struik for PA6 at room temperature [1]. The Unitika nanocomposite has a higher shift rate than the other nanocomposites and unfilled PA6 samples, which may indicate a faster physical ageing. Faster physical ageing can also explain the lower SNC of this nanocomposite as can be seen in Fig. 10.

One important property to take into account when using polyamides is the fact that they absorb moisture from the air, which has a strong influence on the mechanical properties. PA6 absorbs around 2.5% water in a 50% RH environment, which leads to a lowering of T_g of approximately 30 °C [11].

It is particularly interesting to investigate which effect the use of nanofillers has on the creep and physical ageing

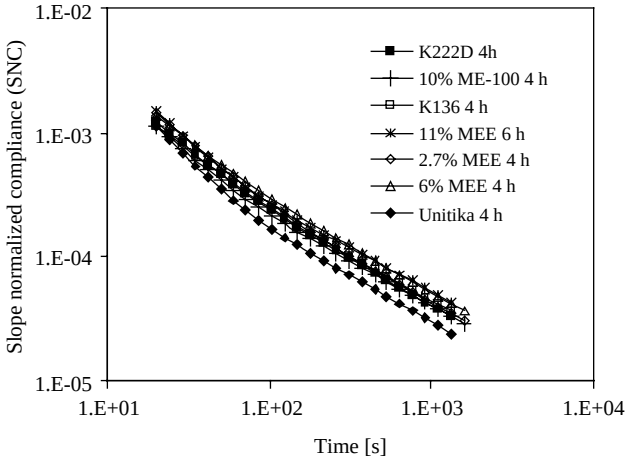

Fig. 10. Slope of the normalized creep compliance curves after 4 h of ageing time (6 h for 11% MEE). Eq. (3) is used for the calculations.

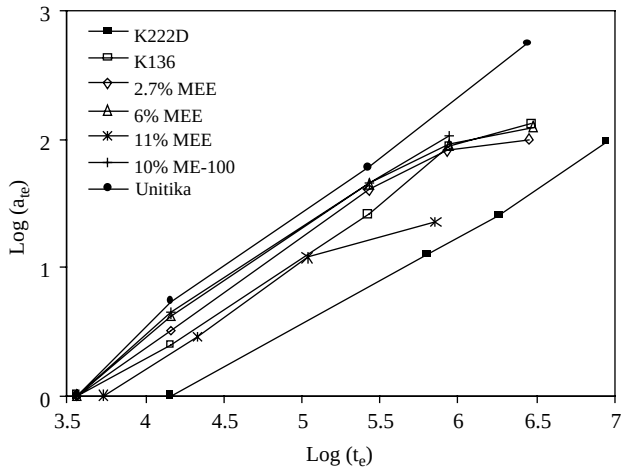

Fig. 11. Double logarithmic plot of the shift factor a_{t_e} versus the ageing time t_e. The slope of the curves is the logarithmic shift rate μ (Table 1).

Table 1
Double logarithmic shift rate

Material	Shift rate μ
K222D	0.70
K136	0.76
2.7% MEE	0.82
6% MEE	0.82
11% MEE	0.83
10% ME-100	0.84
Unitika M1030D	0.93

properties of PA6 nanocomposites in moisture conditioned samples and at elevated temperatures (above T_g). Around T_g the modulus of PA6 shows a steep decrease, and therefore, a strong increase in the creep compliance is expected. It has been shown that the addition of layered silicate nanofillers to PA6 has no significant effect on T_g or on the ultimate moisture absorption capabilities of the polymer [12]. Some results that have been published previously [13] on the creep behavior of moisture conditioned nanocomposites and nanocomposites tested at temperatures above T_g are shown in Fig. 12.

The compliance values in Fig. 12 for dry samples at 23 °C differ slightly from the values in Figs. 1–7, because the applied stress was higher and the ageing was performed for several weeks at 80 °C. The stress in the creep tests in Fig. 12 was approximately 2/3 of the yield stress under the tested conditions, the decrease of the yield stress with increasing temperature and moisture content was taken into account. It can be seen that under these conditions the creep compliance of PA6 is approximately six times higher in moisture-conditioned samples (2.5% water) and 12 times higher in dry samples at 80 °C. However, the addition of nanofillers is very effective in reducing the creep compliance under these conditions, even much more effective than in the dry samples at room temperature. For example, while the addition of 5% MEE nanoparticles results in a reduction of the creep compliance of around 43% in dry samples at 23 °C, in moisture-conditioned samples this is around 63% and in the samples tested at 80 °C it is 83%. The exact physical ageing and creep behavior of PA6 nanocomposites in moisture conditioned samples and at elevated temperatures should be the subject of further research, but these results clearly show the large benefits of PA6 nanocomposites compared to unfilled PA6 under these conditions.

4. Conclusions

The creep compliance is reduced by addition of layered silicate to PA6, as is clear from Fig. 8. The reduction is closely related to the increased modulus of the nanocomposites, which increases with increased ageing time (Fig. 9). The slope of the creep curves decreases strongly (on a linear time scale), which is also evident from the slopes of the normalized creep curves in Fig. 10.

The physical ageing process is not changed much by the addition of the layered silicate, as can be seen from the shape of the creep curves and the shift rate. The shape of the curves is similar in unfilled PA6 and PA6 nanocomposites and the curves for different ageing times can be overlapped onto one master curve by shifts on the time axis, just as in unfilled polymers below T_g. The shift rate is in the same range, although it seems to be slightly higher for nanocomposites (Table 1),

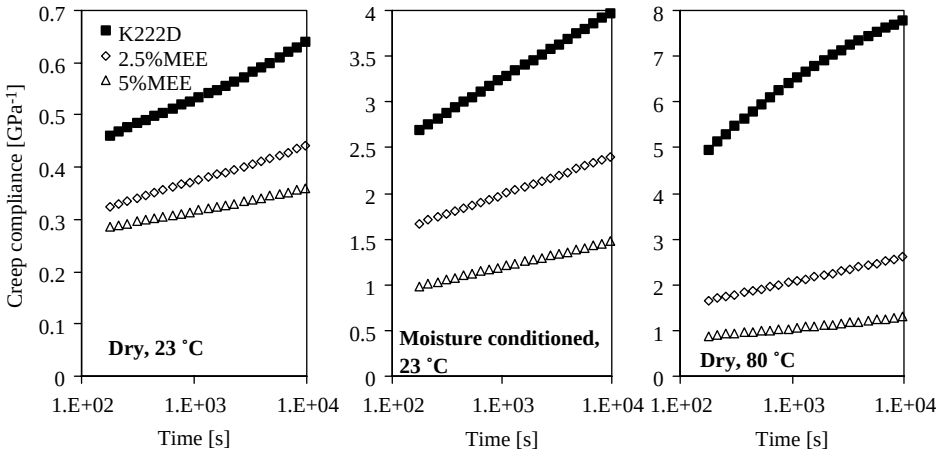

Fig. 12. Effect of absorbed moisture and temperatures above T_g on the creep behavior of PA6 and PA6 nanocomposites.

indicating a slightly faster ageing rate in nanocomposites. In addition, the SNC (Fig. 10) shows little influence of the addition of the nanoparticles.

The creep curves for ageing times longer than one month show a change in shape, and are therefore difficult to overlap on the master curve. It is not clear what the reason is for this change in the shape of the creep curves at very long ageing times.

The creep measurements on PA6 nanocomposites conditioned with an equilibrium amount of moisture and tested at elevated temperatures have shown that the effect of nanofillers is much stronger under these conditions. It has been shown that creep compliances above T_g can be reduced by more than 80% by filling PA6 with 5% of exfoliated silicate. Increasing the temperature from 23 to 80 °C (crossing T_g) only leads to a three times increase of the creep compliance in the 5% silicate nanocomposite, while this is twelve times for unfilled PA6. These results are very important for applications where PA6 is used as load bearing engineering plastic, because with absorption of moisture T_g can decrease below the use temperature and this strongly increases the creep compliance. Further research on the physical ageing behavior of moisture conditioned nanocomposites and nanocomposites at temperatures above T_g is needed to understand the complete time- and temperature-dependent deformation behavior. However, it has been clearly shown that the use of nanocomposites instead of unfilled PA6 can have big advantages for the time dependent deformation behavior.

Acknowledgements

The work of D.P.N. Vlasveld and S.J. Picken forms part of the research program of the Dutch Polymer Institute (DPI), project number 279. The authors would like to thank DSM Research, The Netherlands, for the water-assisted extrusion of the nanocomposites with unmodified silicate.

References

[1] Struik LCE. The mechanical and physical aging of semicrystalline polymers. Part 1. Polymer 1987;28(9):1521–33.
[2] El Shafee E. Effect of aging on the mechanical properties of cold-crystallized poly(trimethylene terephthalate). Polymer 2003;44(13):3727–32.
[3] Spinu I, McKenna GB. Physical aging of nylon-66. Polym Eng Sci 1994;34(24):1808–14.
[4] Struik LCE. Mechanical-behavior and physical aging of semi-crystalline polymers. Part 4. Polymer 1989;30(5):815–30.
[5] Struik LCE. Mechanical-behavior and physical aging of semi-crystalline polymers. Part 3. Prediction of long-term creep from short-time tests. Polymer 1989;30(5):799–814.
[6] Struik LCE. The mechanical-behavior and physical aging of semicrystalline polymers. Part 2. Polymer 1987;28(9):1534–42.
[7] Krishnaswamy RK, Geibel JF, Lewis BJ. Influence of semicrystalline morphology on the physical aging characteristics of poly(phenylene sulfide). Macromolecules 2003;36(8):2907–14.
[8] Beckmann J, McKenna GB, Landes BG, Bank DH, Bubeck RA. Physical aging kinetics of syndiotactic polystyrene as determined from creep behavior. Polym Eng Sci 1997;37(9):1459–68.
[9] Spinu I, McKenna GB. Physical aging of thin films of nylon and PET. J Plast Film Sheeting 1997;13(4):311–26.
[10] Lee A, McKenna GB. Effect of crosslink density on physical aging of epoxy networks. Polymer 1988;29(10):1812–7.
[11] Kohan MI. Nylon plastics handbook. Munich: Carl Hanser Verlag; 1995.
[12] Vlasveld DPN, Bersee HEN, Picken SJ. Moisture absorption in polyamide-6 silicate nanocomposites and its influence on mechanical properties. Polymer 2005; in press; doi: 10.1016/j.polymer.2005.10.096.
[13] Vlasveld DPN, Bersee HEN, Picken SJ. Nanocomposite matrices for continuous fiber reinforced thermoplastic composites. Proceedings of the 25th International SAMPE Europe Conference, Paris 2004 p. 181–6.